NASA TECHNICAL MEMORANDUM

NASA TM X-2837

NASA TM X-2837

PERFORMANCE OF A 1.20-PRESSURE-RATIO STOL FAN STAGE AT THREE ROTOR BLADE SETTING ANGLES

by George W. Lewis, Jr., Royce D. Moore, and George Kovich

Lewis Research Center
Cleveland, Ohio 44135

NATIONAL AERONAUTICS AND SPACE ADMINISTRATION • WASHINGTON, D. C. • JULY 1973

1. Report No. NASA TM X-2837	2. Government Accession No.	3. Recipient's Catalog No.
4. Title and Subtitle PERFORMANCE OF A 1.20-PRESSURE-RATIO STOL FAN STAGE AT THREE ROTOR BLADE SETTING ANGLES		5. Report Date July 1973
		6. Performing Organization Code
7. Author(s) George W. Lewis, Jr., Royce D. Moore, and George Kovich		8. Performing Organization Report No. E-7434
9. Performing Organization Name and Address Lewis Research Center National Aeronautics and Space Administration Cleveland, Ohio 44135		10. Work Unit No. 501-24
		11. Contract or Grant No.
12. Sponsoring Agency Name and Address National Aeronautics and Space Administration Washington, D.C. 20546		13. Type of Report and Period Covered Technical Memorandum
		14. Sponsoring Agency Code
15. Supplementary Notes		

16. Abstract

A 51-centimeter-diameter model of a short takeoff and landing (STOL) fan stage was tested in the Lewis single-stage compressor research facility. This stage was designed and built on contract by the Hamilton Standard Division of United Aircraft Corporation. Surveys of the airflow conditions ahead of the rotor, between the rotor and stator, and behind the stator were made over the stable operating range of the stage. At the design speed of 213.3 meters per second and a weight flow of 31.2 kilograms per second, the stage pressure ratio of 1.15 was less than the design value of 1.2. The stage was tested with the rotor blades reset for more flow. Design pressure ratio was achieved and surpassed with the -5° and -7° resets, respectively. The stage efficiency was 0.88 for the -5° reset and 0.85 for the -7° reset.

17. Key Words (Suggested by Author(s)) Compressors, Turbomachinery, Axial flow, Blade profile, Fans	18. Distribution Statement Unclassified - unlimited

19. Security Classif. (of this report)	20. Security Classif. (of this page)	21. No. of Pages	22. Price*
Unclassified	Unclassified	32	$3.00

* For sale by the National Technical Information Service, Springfield, Virginia 22151

PERFORMANCE OF A 1.20-PRESSURE-RATIO STOL FAN STAGE AT THREE ROTOR BLADE SETTING ANGLES

by George W. Lewis, Jr., Royce D. Moore, and George Kovich

Lewis Research Center

SUMMARY

A 51-centimeter-diameter model of a short takeoff and landing (STOL) fan stage was tested in the Lewis single-stage compressor research facility. This stage was designed and built on contract by the Hamilton Standard Division of United Aircraft Corporation. Surveys of the airflow conditions ahead of the rotor, between the rotor and stator, and behind the stator were made over the stable operating range of the stage. Flow and performance parameters were calculated at the blade leading and trailing edges. Surveys were taken at equivalent rotative speeds of 80, 90, and 100 percent of design speed.

At the design speed of 213.3 meters per second and weight flow of 31.2 kilograms per second (195.3 (kg/sec)/m^2 of annulus area), the stage pressure ratio of 1.15 was less than the design value of 1.2.

The stage was tested with the rotor blade set at a design minus 5° and design minus 7° setting angle. Both setting angles opened the blades for more flow. The design pressure ratio was achieved and surpassed with the -5° and -7° resets, respectively. The stage efficiency was 0.88 for the -5° reset and 0.85 for the -7° reset.

INTRODUCTION

The NASA is currently engaged in investigating short takeoff and landing (STOL) aircraft for commercial application. These aircraft must be dependable and economical, and they must have an efficient and reliable propulsion system that satisfies the low noise requirements of urban communities. The aircraft engines must be capable of a variety of operating conditions from takeoff, cruise and approach to possible thrust reversal on landing.

In support of this program, the Lewis Research Center is investigating a variety of fan stages for STOL engines. The low-pressure-ratio stages suitable for this application must operate at low tip speeds to attain the required low noise level. Adjustable rotor blades may be required to provide the varied flight demands.

This report presents the aerodynamic performance data for a STOL fan stage designed and built under contract for Lewis by the Hamilton Division of the United Aircraft Corporation. The 51-centimeter-diameter fan was designed for a stage pressure ratio of 1.2 and at a tip speed of 213.3 meters per second. The stage was tested with adjustable rotor blades at three different blade setting angles; the design angle and two angles for higher flow. Stage overall performance data are presented for these three configurations. Comparisons of the radial distributions of several flow parameters are also presented.

Aerodynamic Design

The fan stage was designed for a pressure ratio of 1.20, a rotor tip speed of 213.3 meters per second, an efficiency of 0.908, and a weight flow per unit annulus area of 195.3 kilograms per second per square meter. The additional requirements for the fan stage were low noise and adjustable rotor blades. The overall design parameters for this stage (designated stage 55-55) are listed in table I. The selected flow path is presented in figure 1.

The rotor blade used double-circular-arc profiles. The rotor was designed with a tip solidity of 0.89 and a hub-tip radius ratio of 0.46. This resulted in 15 rotor blades with an aspect ratio of 1.43. The stator blades were designed using NACA 400 series airfoils. The constant chord stator blades had a tip solidity of 0.712 and a hub-tip radius ratio of 0.47. The 11 stator blades had an aspect ratio of 1.27.

The blade-element design parameters for rotor 55 and stator 55 are presented in tables II and III, respectively. The blade geometry is given in table IV for the rotor and in table V for the stator. The blade-element design parameters shown are those supplied by the contractor. The symbols and equations are defined in appendixes A and B. The definitions and units used for the tabular data are presented in appendix C.

Compressor Test Facility

The compressor stage was tested in the Lewis single-stage compressor facility, which is described in detail in reference 1 and shown schematically in figure 2. Atmospheric air enters the test facility at an inlet located on the roof of the building and flows through the flow measuring orifice into the plenum chamber upstream of the test stage. The air then passes through the experimental compressor stage into the collector and is exhausted to the facility exhaust system.

Test Stage

The test stage mounted in the research facility is shown in figure 3, and the STOL rotor and stator are shown in figure 4. The 15 rotor blades were machined from a titanium alloy. The rotor blades are assembled with an internal ring gear that allows all blades to be moved simultaneously.

The rotor blade tips were contoured to provide adequate clearance so that the blades could be adjusted to the reverse flow position. The nominal tip clearance at the rotor blade centerline was 0.06 centimeter. At the leading and trailing edges the tip clearances were approximately 0.08 centimeter for the design setting angle. The stator blades were machined from an aluminum alloy. The stators are supported at both the hub and tip.

The stage was tested with both the rotor and stator blades set at design angle (stage 55-55). The stage was also tested with the rotor blades set at two other setting angles that opened the blades for higher flow. The stage configuration with the rotor set at a design minus 7° setting angle has been designated stage 55B-55, and the stage configuration with the rotor set at design minus 5° setting angle has been designated stage 55C-55.

Instrumentation

The compressor weight flow was determined from measurements on a calibrated thin-plate orifice that was 38.9 centimeters in diameter. The orifice temperature was determined from an average of two chromel-constantan thermocouples. Orifice pressures were measured by calibrated transducers.

Radial surveys of the flow were made upstream of the rotor, between the rotor and stator, and downstream of the stator (see fig. 1 for axial location). Total pressure, total temperature, and flow angle were measured with the combination probe (fig. 5(a)), and the static pressure was measured with a 8° C-shaped wedge probe (fig. 5(b)). Each probe was positioned with a null-balancing, stream-directional, sensitive control system that automatically alined the probe to the direction of flow. The thermocouple material was chromel-constantan. Two combination probes and two wedge static probes were used at each of the three measuring stations.

Inner and outer wall static-pressure taps were located at approximately the same axial stations as the survey probes. The circumferential locations of both types of survey probes along with inner and outer wall static-pressure taps are shown in figure 6.

An electronic speed counter, in conjunction with a magnetic pickup, was used to measure rotative speed (rpm).

The estimated errors of the data, based on inherent accuracies of the instrumentation and recording system, are as follows:

Flow rate, kg/sec	±0.3
Rotative speed, rpm	±30
Flow angle, deg	±1
Temperature, K	±0.6
Rotor-inlet total pressure, N/cm^2	±0.01
Rotor-outlet total pressure, N/cm^2	±0.10
Stator-outlet total pressure, N/cm^2	±0.10
Rotor-inlet static pressure, N/cm^2	±0.04
Rotor-outlet static pressure, N/cm^2	±0.07
Stator-outlet static pressure, N/cm^2	±0.07

Test Procedure

The stage survey data were taken over a range of weight flow from maximum flow to the near-stall conditions. At 80, 90, and 100 percent of design speed, radial surveys were taken at five or more weight flows. Data were recorded at nine radial positions for each speed and weight flow.

At each radial position the two combination probes behind the stator were circumferentially traversed to nine different locations across the stator gap. The wedge probes were set at midgap because preliminary studies showed that the static pressure across the stator gap was constant. Values of total pressure, total temperature, and flow angle were recorded at each circumferential position. At the last circumferential position, values of pressure, temperature, and flow angle were also recorded at stations 1 and 2. All probes were then moved to the next radial position, and the circumferential traverse procedure repeated.

At each of the three rotative speeds the back pressure on the stage was increased by closing the sleeve valve in the collector until stall was detected by a sudden drop in stage outlet total pressure. This pressure was measured by a probe located at midpassage, downstream of stators, and was recorded on an X-Y plotter. Stall was corroborated by large increases in the measured blade stresses on the rotor with a sudden increase in noise level.

Calculation Procedure

Measured total temperatures and total pressures were corrected for Mach number and streamline slope. These corrections were based on the instrument probe calibrations given in reference 2. The stream static pressure was corrected for Mach number and streamline slope based on an average calibration for the type of probe used.

Because of the physical construction of the C-shaped static-pressure wedges, it was not possible to obtain static-pressure measurements at 5, 10, and 95 percent of span from the rotor tip. The static pressure at 95 percent span was obtained by assuming a linear variation in static pressure between the values at the inner wall and the probe measurement at 90 percent span. A similar variation was assumed between the static-pressure measurements at the outer wall and the 15-percent span position to obtain the static pressure at 5 and 10 percent span positions.

At each radial position, averaged values of the nine circumferential measurements of pressure, temperature rise, and flow angle downstream of the stator (station 3) were obtained. The nine values of total temperature were mass averaged to obtain the stage total-temperature rise. The nine values of total pressure were energy averaged. The measured values of pressure, temperature, and flow angle were used to calculate axial and tangential velocities at each circumferential position. The flow angles presented for each radial position are calculated based on these mass-averaged axial and tangential velocities. To obtain the overall performance, the radial values of total temperature were mass averaged, and the values of total pressure were energy averaged. At each measuring station the integrated weight flow was computed based on the radial survey data.

The data, measured at the three measuring stations, have been translated to planes approximating the blade leading and trailing edges by the method presented in reference 3.

The weight flow at stall was obtained in the following manner: During operation in the near-stall condition, the collector valve was slowly closed in small increments and the weight flow was obtained. The weight flow obtained just before stall occurred is called the stall weight flow. The pressure ratio at stall was obtained by extrapolating the total pressure obtained from the survey data to the stall weight flow.

Orifice weight flow, total pressures, static pressures, and temperatures were all corrected to sea-level conditions based on the rotor-inlet conditions.

RESULTS AND DISCUSSION

The results of this investigation are presented in two main sections. First, the overall performance of the rotor and stage are presented for the three different configurations. The radial distribution of several performance parameters are then to be compared with the design values for both the rotor and stator at the design setting angle.

Overall Performance

The overall performance for the rotor and stage configurations are presented in figures 7 and 8, respectively. Pressure ratio, temperature ratio, and efficiency are presented at several values of weight flow, from choking flow to stall, for 80, 90, and 100 percent design speeds. The solid symbols represent the design values.

Rotor Performance

At the design setting angle the rotor is operating near peak efficiency at the design flow of 31.2 kilograms per second (fig. 7(a)); however, both pressure ratio and temperature ratio are considerably less than the design values. The flow range at the design setting angle is from 25 to 33 kilograms per second at design speed. The peak efficiency was 0.918 at design speed.

To obtain the design pressure ratio at design flow, the rotor blades were reset to the design setting angle minus 7° and minus 5°. Both setting angles moved the blade toward an axial orientation, increasing the throat area. At design speed and weight flow, pressure ratios of 1.21 and 1.22 were obtained for the blade setting angles of design minus 5° and minus 7°, respectively. Maximum efficiencies greater than 0.90 were obtained for both of these angle settings.

Stage Performance

The design pressure ratio for the stage was attained at design speed for the design minus 5° rotor setting angle (fig. 8(b)). A comparison of the rotor and stage efficiency curves indicates that the rotor and stator were also better matched at this setting angle. Peak efficiencies (rotor and stage of 0.90 and 0.88, respectively) are obtained at approximately design weight flow.

At the rotor setting angle of design minus 7°, a somewhat higher pressure ratio was obtained at some cost in efficiency at design flow and speed. Maximum stall margin for the stage is obtained for the design minus 5° rotor blade angle; it is 19.5 percent based on the weight flow and total pressure ratio at peak efficiency and near stall.

Radial Distribution of Performance

The radial variations of several blade-element and performance parameters for both the design and the design minus 5° rotor setting angles at design speed and near design flow are presented for the rotors in figure 9 and for the stators in figure 10. Design values are indicated as dashed lines in the figures.

Rotor. - For the design rotor setting angle (fig. 9) both total-pressure ratio and temperature ratio are slightly less than design values over the blade height. Deviation angles are about 2° greater than design over the outer half of the rotor blade height. Incidence angles compare closely with design.

At the design minus 5° rotor blade setting angle, the total-pressure ratio and total-temperature ratio values agree favorably with design. The difference in work input (total-temperature ratio) and total-pressure ratio between the rotor with the design setting angle and that with the design minus 5° setting angle are reasonably uniform over the blade height. The efficiency profiles for the two setting angles are practically identical from the 30-percent span station to the hub. Efficiency decreases with the lower setting angle in the tip region. The incidence angle for the rotor design setting angle agrees closely with the design values. Deviation angle for the design minus 5° rotor setting angle is somewhat greater than the design values in the tip region but less than design values in the hub region.

Stator. - The radial variations of meridional velocity ratio, mean incidence angle, and deviation angle at the stator exit are shown in figure 10. The stator blades are set at the design angle, and the data are for design peak efficiency performance with the design angle and the design angle minus 5° rotor blade setting angles.

Because of the physical dimensions of the test facility, the survey station downstream of the stator was relatively close to the blade trailing edges. The relatively strong circumferential velocity gradients at this station apparently introduced inaccuracies, particularly in the measured flow angle. The integrated mass flow at station 3 was generally 6 to 12 percent higher than the orifice-measured flow, whereas at stations 1 and 2 the percentages were, respectively, averaging only 1.5 and 4.0 percent higher. Nevertheless, the measured values of total temperature and total pressure downstream of the stator appears to be reasonable compared with survey results at the rotor exit.

With the rotor operating at design minus 5° setting angle, the mean stator incidence angle matches design values fairly closely over most of the blade height but are less negative than the design values in the hub region. Measured deviation angles are consistently lower than the design values so that the stator tends to turn the flow past the axial direction. The measured meridional velocity ratio data indicate less than design diffusion in the hub region.

SUMMARY OF RESULTS

This report presents the overall and blade-element performance of a STOL fan stage with rotor blades set at the design angle, design angle minus 7°, and at design angle minus 5°. Radial surveys of the flow conditions at the rotor blade inlet and outlet were made over the stage stable operating flow range at equivalent rotating speeds of 80, 90, and 100 percent design speed. Both radial and circumferential surveys of the flow conditions were taken at the stator outlet. Flow and performance parameters were calculated at a number of selected blade elements. The following principal results were obtained:

1. With the rotor blades set at an angle of design minus 5°, the design stage pressure ratio of 1.2 was obtained with a design flow of 31.2 kilograms per second at a tip speed of 213.3 meters per second. Measured efficiency was 0.88.
2. Stall margin for the design minus 5° rotor setting angle at design speed was 19.5 percent based on the weight flow and total-pressure ratio at peak efficiency and near stall.
3. Radial distributions of total pressure and total-temperature ratio downstream of the rotor agree favorably with design values for a rotor blade setting angle of design minus 5°. These values for the design rotor setting angle were only slightly lower.

Lewis Research Center,
National Aeronautics and Space Administration,
Cleveland, Ohio, May 10, 1973,
501-24.

APPENDIX A

SYMBOLS

A_{an}	annulus area at rotor leading edge, 0.160 m^2
A_f	frontal area at rotor leading edge, 0.203 m^2
C_p	specific heat at constant pressure, 1004 (J/kg)/K
D	diffusion factor
g	acceleration of gravity, 9.8 m/sec^2
i_{mc}	mean incidence angle, angle between inlet air direction and line tangent to blade mean camber line at leading edge, deg
i_{ss}	suction-surface incidence angle, angle between inlet air direction and line tangent to blade suction surface at leading edge, deg
J	mechanical equivalent of heat
N	rotative speed, rpm
P	total pressure, N/cm^2
p	static pressure, N/cm^2
r	radius, cm
SM	stall margin
T	total temperature, K
U	wheel speed, m/sec
V	air velocity, m/sec
W	weight flow, kg/sec
Z	axial distance referenced from rotor-blade-hub leading edge, cm
β	air angle, angle between air velocity and axial direction, deg
β'_c	relative meridional air angle based on cone angle, arctan ($\tan \beta'_m \cos \alpha_c / \cos \alpha_s$), deg
γ	ratio of specific heats, 1.40
γ_b	blade setting angle
δ	ratio of rotor-inlet total pressure to standard pressure of 10.13 N/cm^2

δ^{o} deviation angle, angle between exit air direction and tangent to blade mean camber line at trailing edge, deg

θ ratio of rotor-inlet total temperature to standard temperature of 288.2 K

η efficiency

κ_{mc} angle between blade mean camber line and meridional plane, deg

κ_{ss} angle between blade suction-surface camber line at leading edge and meridional plane, deg

σ solidity, ratio of chord to spacing

$\overline{\omega}$ total loss coefficient

$\overline{\omega}_p$ profile loss coefficient

$\overline{\omega}_s$ shock loss coefficient

Subscripts:

ad adiabatic (temperature rise)

id ideal

LE blade leading edge

m meridional direction

mom momentum rise

r radial direction

ref reference

stall stall

TE blade trailing edge

θ tangential direction

1 instrumentation plane upstream of rotor

2 instrumentation plane between rotor and stator

3 instrumentation plane downstream of stator

Superscript:

' relative to blade

APPENDIX B

PERFORMANCE PARAMETERS

The performance parameters referred to in the main text are defined by the equations or expressions in this appendix.

Incidence angle based on suction-surface blade angle:

$$i_{ss} = \left(\beta'_c\right)_{LE} - \left(\kappa_{ss}\right)_{LE} \tag{B1}$$

Incidence angle based on mean blade angle:

$$i_{mc} = \left(\beta'_c\right)_{LE} - \left(\kappa_{mc}\right)_{LE} \tag{B2}$$

Deviation:

$$\delta^o = \left(\beta'_c\right)_{TE} - \left(\kappa_{mc}\right)_{TE} \tag{B3}$$

Diffusion factor:

$$D = 1 - \frac{V'_{TE}}{V'_{LE}} + \frac{\left(rV_\theta\right)_{TE} - \left(rV_\theta\right)_{LE}}{\left(r_{LE} + r_{TE}\right)\sigma V'_{LE}} \tag{B4}$$

Total loss coefficient:

$$\overline{\omega} = \frac{\left(P'_{id}\right)_{TE} - P'_{TE}}{P'_{LE} - p_{LE}} \tag{B5}$$

Profile loss coefficient:

$$\overline{\omega}_p = \overline{\omega} - \overline{\omega}_s \tag{B6}$$

Total loss parameter:

$$\frac{\overline{\omega} \cos \left(\beta'_m\right)_{TE}}{2\sigma} \tag{B7}$$

Profile loss parameter:

$$\frac{(\omega - \omega_s) \cos \left(\beta'_m\right)_{TE}}{2\sigma} \tag{B8}$$

Adiabatic efficiency:

$$\eta_{ad} = \frac{\left(\frac{P_{TE}}{P_{LE}}\right)^{(\gamma-1)/\gamma} - 1}{\frac{T_{TE}}{T_{LE}} - 1} \tag{B9}$$

Stall margin:

$$SM = \left[\frac{\left(\frac{P_{TE}}{P_{LE}}\right)_{stall}}{\left(\frac{P_{TE}}{P_{LE}}\right)_{ref}} \frac{\left(\frac{W\sqrt{\theta}}{\delta}\right)_{ref}}{\left(\frac{W\sqrt{\theta}}{\delta}\right)_{stall}} - 1\right] \times 100 \tag{B10}$$

Momentum rise efficiency:

$$\eta_{mom} = \frac{\left(\frac{P_{TE}}{P_{LE}}\right)^{(\gamma-1)/\gamma} - 1}{\frac{\left(UV_\theta\right)_{TE} - \left(UV_\theta\right)_{LE}}{T_{LE} gJC_p}} \tag{B11}$$

Equivalent weight flow:

$$\frac{W\sqrt{\theta}}{\delta} \tag{B12}$$

Equivalent rotative speed:

$$\frac{N}{\sqrt{\theta}} \tag{B13}$$

Equivalent weight flow per unit annulus area:

$$\frac{w\sqrt{\theta}}{A_{an}\delta} \tag{B14}$$

Equivalent weight flow per unit frontal area:

$$\frac{w\sqrt{\theta}}{A_{f}\delta} \tag{B15}$$

APPENDIX C

DEFINITIONS AND UNITS USED IN TABLES

ABS	absolute
AERO CHORD	aerodynamic chord, cm
AREA RATIO	ratio of actual flow area to critical area (where local Mach number is 1)
BETAM	meridional air angle, deg
CONE ANGLE	angle between axial direction and conical surface representing blade element, deg
DELTA INC	difference between mean camber blade angle and suction-surface blade angle, deg
DEV	deviation angle (defined by eq. (B3)), deg
D-FACT	diffusion factor (defined by eq. (B4))
EFF	adiabatic efficiency (defined by eq. (B9))
IN	inlet (leading edge of blade)
INCIDENCE	incidence angle (suction surface defined by eq. (B1) and mean defined by eq. (B2))
KIC	angle between blade mean camber line and meridional plane at leading edge, deg
KOC	angle between blade mean camber line and meridional plane at trailing edge, deg
KTC	angle between blade mean camber line and meridional plane at transition point, deg
LOSS COEFF	loss coefficient (total defined by eq. (B5) and profile defined by eq. (B6))
LOSS PARAM	loss parameter (total defined by eq. (B7) and profile defined by eq. (B8))
MERID	meridional
MERID VEL R	meridional velocity ratio
OUT	outlet (trailing edge of blade)
PERCENT SPAN	percent of blade span from tip at rotor outlet

PHISS	suction-surface camber ahead of assumed shock location, deg
PRESS	pressure, N/cm^2
PROF	profile
RADII	radius, cm
REL	relative to blade
RI	inlet radius (leading edge of blade), cm
RO	outlet radius (trailing edge of blade), cm
RP	radial position
RPM	equivalent rotative speed, rpm
SETTING ANGLE	angle between aerodynamic chord and meridional plane, deg
SOLIDITY	ratio of aerodynamic chord to blade spacing
SPEED	speed, m/sec
SS	suction surface
STREAMLINE SLOPE	slope of streamline, deg
TANG	tangential
TEMP	temperature, K
TI	thickness of blade at leading edge, cm
TM	thickness of blade at maximum thickness, cm
TO	thickness of blade at trailing edge, cm
TOT	total
TOTAL CAMBER	difference between inlet and outlet blade mean camber line, deg
VEL	velocity, m/sec
WT FLOW	equivalent weight flow, kg/sec
X FACTOR	ratio of suction-surface camber ahead of assumed shock location of multiple-circular-arc blade section to that of double-circular-arc blade section
ZMC	axial distance to blade maximum thickness point from inlet, cm
ZOC	axial distance to blade trailing edge from inlet, cm
ZTC	axial distance to transition point from inlet, cm
ZI	axial distance to blade leading edge from inlet, cm

REFERENCES

1. Urasek, Donald C.; and Janetzke, David C.: Performance of Tandem-Bladed Transonic Compressor Rotor with Tip Speed of 1375 Feet per Second. NASA TM X-2484, 1972.

2. Glawe, George E.; Krause, Lloyd N.; and Dudzinski, Thomas J.: A Small Combination Sensing Probe for Measurement of Temperature, Pressure, and Flow Direction. NASA TN D-4816, 1968.

3. Ball, Calvin L.; Janetzke, David C.; and Reid, Lonnie: Performance of 1380 Foot Per Second Tip-Speed Axial-Flow Compressor Rotor Blade Tip Solidity of 1.5. NASA TM X-2379, 1972.

TABLE I. - DESIGN OVERALL PARAMETERS

FOR STAGE 55-55

ROTOR TOTAL PRESSURE RATIO	1.205
STAGE TOTAL PRESSURE RATIO	1.196
ROTOR TOTAL TEMPERATURE RATIO.	1.058
STAGE TOTAL TEMPERATURE RATIO.	1.058
ROTOR ADIABATIC EFFICIENCY	0.940
STAGE ADIABATIC EFFICIENCY	0.903
ROTOR POLYTROPIC EFFICIENCY.	0.941
STAGE POLYTROPIC EFFICIENCY.	0.906
ROTOR HEAD RISE COEFFICIENT	0.348
STAGE HEAD RISE COEFFICIENT	0.334
FLOW COEFFICIENT.	0.861
WT FLOW PER UNIT FRONTAL AREA	153.970
WT FLOW PER UNIT ANNULUS AREA	195.295
WT FLOW	31.207
RPM	8020.000
TIP SPEED	213.323

TABLE II. - DESIGN BLADE-ELEMENT PARAMETERS FOR ROTOR 55

RP	RADII IN	RADII OUT	ABS BETAM IN	ABS BETAM OUT	REL BETAM IN	REL BETAM OUT	TOTAL TEMP IN	TOTAL TEMP RATIO	TOTAL PRESS IN	TOTAL PRESS RATIO
TIP	25.400	25.400	0.	27.6	48.4	38.1	288.2	1.063	10.14	1.213
1	24.730	24.714	0.	28.8	47.8	34.9	288.2	1.065	10.14	1.226
2	24.026	24.028	-0.	29.7	47.2	32.1	288.2	1.067	10.14	1.235
3	23.323	23.343	-0.	30.4	46.5	29.7	288.2	1.067	10.14	1.238
4	21.172	21.285	-0.	31.6	44.1	24.1	288.2	1.064	10.14	1.231
5	18.320	18.542	-0.	32.9	40.2	16.6	288.2	1.057	10.14	1.208
6	15.539	15.799	-0.	34.7	35.7	7.9	288.2	1.051	10.14	1.178
7	13.541	13.741	-0.	36.1	32.0	1.4	288.2	1.044	10.14	1.144
8	12.907	13.056	-0.	36.6	30.7	-0.7	288.2	1.042	10.14	1.130
9	12.288	12.370	-0.	37.1	29.4	-2.8	288.2	1.040	10.14	1.115
HUB	11.684	11.684	0.	37.6	28.1	-4.8	288.2	1.037	10.14	1.098

RP	ABS VEL IN	ABS VEL OUT	REL VEL IN	REL VEL OUT	MERID VEL IN	MERID VEL OUT	TANG VEL IN	TANG VEL OUT	WHEEL SPEED IN	WHEEL SPEED OUT
TIP	189.4	184.1	285.3	207.3	189.4	163.1	0.	85.3	213.3	213.3
1	188.1	190.0	280.2	203.0	188.1	166.5	0.	91.5	207.7	207.6
2	186.9	194.1	275.0	198.9	186.9	168.6	-0.	96.2	201.8	201.8
3	185.9	196.3	270.1	194.9	185.9	169.3	-0.	99.4	195.9	196.0
4	183.6	197.6	255.6	184.4	183.6	168.3	-0.	103.6	177.8	178.8
5	181.8	196.3	238.2	172.0	181.8	164.8	-0.	106.6	153.9	155.7
6	181.3	194.5	223.4	161.4	181.3	159.9	-0.	110.6	130.5	132.7
7	182.0	189.8	214.7	153.5	182.0	153.5	-0.	111.7	113.7	115.4
8	182.6	187.2	212.3	150.4	182.6	150.4	-0.	111.5	108.4	109.6
9	183.2	184.1	210.3	147.0	183.2	146.9	-0.	111.0	103.2	103.9
HUB	183.9	180.4	208.5	143.4	183.9	142.9	0.	110.2	98.1	98.1

RP	ABS MACH NO IN	ABS MACH NO OUT	REL MACH NO IN	REL MACH NO OUT	MERID MACH NO IN	MERID MACH NO OUT	STREAMLINE SLOPE IN	STREAMLINE SLOPE OUT	MERID VEL R	PEAK SS MACH NO
TIP	0.575	0.540	0.865	0.608	0.575	0.478	0.78	0.46	0.861	0.865
1	0.570	0.557	0.850	0.595	0.570	0.488	0.66	0.55	0.885	0.850
2	0.567	0.570	0.834	0.584	0.567	0.495	0.61	0.66	0.902	0.834
3	0.563	0.577	0.818	0.573	0.563	0.497	0.62	0.79	0.911	0.818
4	0.556	0.582	0.774	0.543	0.556	0.496	0.85	1.14	0.917	0.774
5	0.550	0.579	0.721	0.508	0.550	0.487	1.26	1.43	0.907	0.721
6	0.549	0.576	0.676	0.478	0.549	0.473	1.39	1.40	0.882	0.676
7	0.551	0.563	0.650	0.455	0.551	0.455	1.04	0.98	0.843	0.650
8	0.553	0.555	0.643	0.446	0.553	0.446	0.78	0.71	0.824	0.643
9	0.555	0.546	0.637	0.436	0.555	0.436	0.44	0.37	0.802	0.637
HUB	0.557	0.535	0.631	0.425	0.557	0.424	0.05	-0.03	0.777	0.635

RP	PERCENT SPAN	INCIDENCE MEAN	DEV	D-FACT	EFF	LOSS COEFF TOT	LOSS COEFF PROF	LOSS PARAM TOT	LOSS PARAM PROF
TIP	0.	-2.0	6.1	0.441	0.903	0.051	0.051	0.023	0.023
1	5.00	-2.4	7.2	0.458	0.917	0.047	0.047	0.022	0.022
2	10.00	-2.9	8.0	0.470	0.928	0.043	0.043	0.020	0.020
3	15.00	-3.2	8.5	0.479	0.936	0.039	0.039	0.019	0.019
4	30.00	-3.6	10.5	0.493	0.958	0.027	0.027	0.013	0.013
5	50.00	-3.7	12.2	0.503	0.970	0.019	0.019	0.009	0.009
6	70.00	-3.9	12.6	0.512	0.949	0.032	0.032	0.015	0.015
7	85.00	-2.4	12.4	0.517	0.884	0.070	0.070	0.031	0.031
8	90.00	-1.7	12.3	0.520	0.844	0.090	0.090	0.039	0.039
9	95.00	-0.9	12.2	0.524	0.792	0.116	0.116	0.049	0.049
HUB	100.00	0.0	12.0	0.529	0.724	0.145	0.145	0.059	0.059

TABLE III. - DESIGN BLADE-ELEMENT PARAMETERS FOR STATOR 55

	RADII		ABS BETAM		REL BETAM		TOTAL TEMP		TOTAL PRESS	
RP	IN	OUT	IN	OUT	IN	OUT	IN	RATIO	IN	RATIO
TIP	25.938	25.938	27.9	-0.	27.9	-0.	306.2	1.000	12.29	0.992
1	25.231	25.299	28.9	0.	28.9	0.	307.0	1.000	12.43	0.992
2	24.547	24.672	29.7	-0.	29.7	-0.	307.5	1.000	12.51	0.993
3	23.877	24.048	30.3	-0.	30.3	-0.	307.5	1.000	12.55	0.994
4	21.847	22.222	31.2	-0.	31.2	-0.	306.6	1.000	12.48	0.997
5	19.166	19.826	32.3	-0.	32.3	-0.	304.7	1.000	12.24	0.996
6	16.502	17.464	34.0	-0.	34.0	-0.	302.7	1.000	11.94	0.991
7	14.518	15.682	35.4	-0.	35.4	-0.	301.0	1.000	11.60	0.985
8	13.859	15.069	35.9	-0.	35.9	-0.	300.3	1.000	11.45	0.982
9	13.202	14.447	36.4	-0.	36.4	-0.	299.6	1.000	11.30	0.979
HUB	12.548	13.818	36.9	0.	36.9	0.	298.9	1.000	11.13	0.976

	ABS VEL		REL VEL		MERID VEL		TANG VEL		WHEEL SPEED	
RP	IN	OUT	IN	OUT	IN	OUT	IN	OUT	IN	OUT
TIP	178.6	169.2	178.6	169.2	157.9	169.2	83.5	-0.	0.	0.
1	185.4	175.1	185.4	175.1	162.3	175.1	89.6	0.	0.	0.
2	190.0	178.9	190.0	178.9	165.1	178.9	94.1	-0.	0.	0.
3	192.7	180.8	192.7	180.8	166.5	180.8	97.2	-0.	0.	0.
4	194.8	179.9	194.8	179.9	166.7	179.9	100.9	-0.	0.	0.
5	193.0	172.7	193.0	172.7	163.1	172.7	103.1	-0.	0.	0.
6	189.3	160.6	189.3	160.6	156.9	160.6	105.9	-0.	0.	0.
7	182.6	143.7	182.6	143.7	148.9	143.7	105.8	-0.	0.	0.
8	179.3	135.4	179.3	135.4	145.3	135.4	105.0	-0.	0.	0.
9	175.3	125.7	175.3	125.7	141.2	125.7	104.0	-0.	0.	0.
HUB	170.9	114.6	170.9	114.6	136.6	114.6	102.6	0.	0.	0.

	ABS MACH NO		REL MACH NO		MERID MACH NO		STREAMLINE SLOPE		MERID	PEAK SS
RP	IN	OUT	IN	OUT	IN	OUT	IN	OUT	VEL R	MACH NO
TIP	0.523	0.494	0.523	0.494	0.462	0.494	0.63	-0.10	1.071	0.523
1	0.543	0.511	0.543	0.511	0.475	0.511	0.86	0.05	1.079	0.543
2	0.557	0.523	0.557	0.523	0.484	0.523	1.10	0.22	1.084	0.557
3	0.566	0.528	0.566	0.528	0.488	0.528	1.34	0.39	1.086	0.566
4	0.573	0.526	0.573	0.526	0.490	0.526	2.08	0.95	1.079	0.573
5	0.569	0.506	0.569	0.506	0.481	0.506	3.13	1.72	1.058	0.569
6	0.559	0.471	0.559	0.471	0.464	0.471	4.25	2.42	1.024	0.559
7	0.540	0.420	0.540	0.420	0.440	0.420	5.10	2.77	0.965	0.540
8	0.530	0.396	0.530	0.396	0.430	0.396	5.35	2.76	0.932	0.530
9	0.519	0.367	0.519	0.367	0.418	0.367	5.58	2.68	0.890	0.519
HUB	0.505	0.334	0.505	0.334	0.404	0.334	5.80	2.54	0.839	0.505

	PERCENT	INCIDENCE	DEV	D-FACT	EFF	LOSS COEFF		LOSS PARAM	
RP	SPAN	MEAN				TOT	PROF	TOT	PROF
TIP	0.	-12.5	16.0	0.380	0.	0.049	0.049	0.034	0.034
1	5.00	-11.6	15.6	0.385	0.	0.042	0.042	0.029	0.029
2	10.00	-10.9	15.3	0.386	0.	0.036	0.036	0.024	0.024
3	15.00	-10.3	15.0	0.387	0.	0.030	0.030	0.019	0.019
4	30.00	-9.8	14.0	0.382	0.	0.017	0.017	0.010	0.010
5	50.00	-9.1	13.0	0.382	0.	0.018	0.018	0.010	0.010
6	70.00	-7.8	11.7	0.400	0.	0.046	0.046	0.021	0.021
7	85.00	-6.8	10.9	0.440	0.	0.086	0.086	0.035	0.035
8	90.00	-6.4	10.7	0.464	0.	0.103	0.103	0.040	0.040
9	95.00	-6.0	10.4	0.494	0.	0.123	0.123	0.046	0.046
HUB	100.00	-5.6	10.1	0.533	0.	0.147	0.147	0.052	0.052

TABLE IV. - BLADE GEOMETRY FOR ROTOR 55

RP	PERCENT SPAN	RADII RI	RO	BLADE ANGLES KIC	KTC	KOC	CONE ANGLE
TIP	0.	25.400	25.400	50.40	41.08	32.00	0.057
1	5.	24.730	24.714	50.29	38.96	27.64	-0.124
2	10.	24.026	24.028	50.05	37.05	24.05	0.057
3	15.	23.323	23.343	49.67	35.44	21.21	0.152
4	30.	21.172	21.285	47.72	30.64	13.56	0.892
5	50.	18.320	18.542	43.95	24.18	4.41	1.806
6	70.	15.539	15.799	39.62	17.42	-4.79	2.239
7	85.	13.541	13.741	34.40	11.69	-11.02	1.813
8	90.	12.907	13.056	32.39	9.69	-13.01	1.375
9	95.	12.288	12.370	30.27	7.66	-14.95	0.769
HUB	100.	11.684	11.684	28.06	5.61	-16.84	0.057

RP	BLADE THICKNESSES TI	TM	TO	AXIAL DIMENSIONS ZI	ZMC	ZTC	ZO
TIP	0.019	0.239	0.019	-0.636	2.690	2.690	6.522
1	0.025	0.264	0.025	-0.671	2.650	2.650	6.546
2	0.031	0.293	0.031	-0.685	2.639	2.639	6.588
3	0.036	0.326	0.036	-0.680	2.658	2.658	6.644
4	0.050	0.441	0.050	-0.659	2.648	2.648	6.597
5	0.063	0.591	0.063	-0.572	2.669	2.669	6.455
6	0.083	0.741	0.083	-0.371	2.753	2.753	6.284
7	0.091	0.839	0.091	-0.206	2.824	2.824	6.116
8	0.090	0.862	0.090	-0.142	2.852	2.852	6.057
9	0.088	0.881	0.088	-0.073	2.881	2.881	5.998
HUB	0.084	0.896	0.084	0.	2.912	2.912	5.938

RP	AERO CHORD	SETTING ANGLE	TOTAL CAMBER	SOLIDITY	X FACTOR
TIP	9.499	41.14	18.40	0.893	1.000
1	9.274	38.96	22.65	0.896	1.000
2	9.105	37.05	26.00	0.905	1.000
3	8.980	35.44	28.47	0.919	1.000
4	8.428	30.66	34.15	0.948	1.000
5	7.703	24.22	39.54	0.998	1.000
6	6.978	17.48	44.41	1.063	1.000
7	6.458	11.74	45.42	1.130	1.000
8	6.290	9.73	45.40	1.157	1.000
9	6.126	7.69	45.22	1.186	1.000
HUB	5.966	5.61	44.89	1.219	1.000

TABLE V. - BLADE GEOMETRY FOR STATOR 55

RP	PERCENT SPAN	RADII RI	RO	BLADE ANGLES KIC	KTC	KOC	CONE ANGLE
TIP	0.	25.938	25.938	40.40	17.86	-16.01	0.057
1	5.	25.231	25.299	40.47	18.05	-15.65	0.378
2	10.	24.547	24.672	40.54	18.23	-15.31	0.693
3	15.	23.877	24.048	40.61	18.40	-14.98	0.952
4	30.	21.847	22.222	41.00	19.02	-14.04	2.087
5	50.	19.166	19.826	41.42	19.69	-13.02	3.692
6	70.	16.502	17.464	41.78	20.44	-11.73	5.406
7	85.	14.518	15.682	42.13	20.97	-10.93	6.564
8	90.	13.859	15.069	42.23	21.15	-10.66	6.832
9	95.	13.202	14.447	42.32	21.32	-10.38	7.039
HUB	100.	12.548	13.818	42.40	21.48	-10.10	7.185

RP	BLADE THICKNESSES TI	TM	TO	AXIAL DIMENSIONS ZI	ZMC	ZTC	ZO
TIP	0.188	0.953	0.087	21.634	25.502	25.502	31.982
1	0.188	0.953	0.087	21.628	25.489	25.489	31.967
2	0.188	0.953	0.087	21.631	25.486	25.486	31.961
3	0.188	0.953	0.087	21.642	25.490	25.490	31.963
4	0.188	0.953	0.087	21.650	25.473	25.473	31.937
5	0.188	0.953	0.087	21.662	25.453	25.453	31.899
6	0.188	0.953	0.087	21.673	25.426	25.426	31.844
7	0.188	0.953	0.087	21.681	25.404	25.404	31.800
8	0.188	0.953	0.087	21.684	25.398	25.398	31.787
9	0.188	0.953	0.087	21.686	25.392	25.392	31.775
HUB	0.188	0.953	0.087	21.689	25.387	25.387	31.764

RP	AERO CHORD	SETTING ANGLE	TOTAL CAMBER	SOLIDITY
TIP	10.584	11.92	56.40	0.714
1	10.584	12.15	56.12	0.733
2	10.584	12.36	55.85	0.753
3	10.584	12.57	55.59	0.773
4	10.584	13.28	55.04	0.841
5	10.585	14.07	54.44	0.951
6	10.586	15.00	53.51	1.091
7	10.588	15.67	53.06	1.228
8	10.588	15.88	52.88	1.282
9	10.589	16.09	52.69	1.341
HUB	10.589	16.30	52.50	1.406

Axial location, z, cm	Hub	Tip
	Radius, r, cm	
-15	7.8	26.0
-10	10.4	26.0
-5	11.5	25.7
0	11.55	25.4
5	11.55	25.4
10	11.60	25.4
15	11.85	25.6
20	12.25	25.85
25	12.55	25.94
30	13.10	
35	13.90	
40	13.40	
45	13.00	
50	12.50	

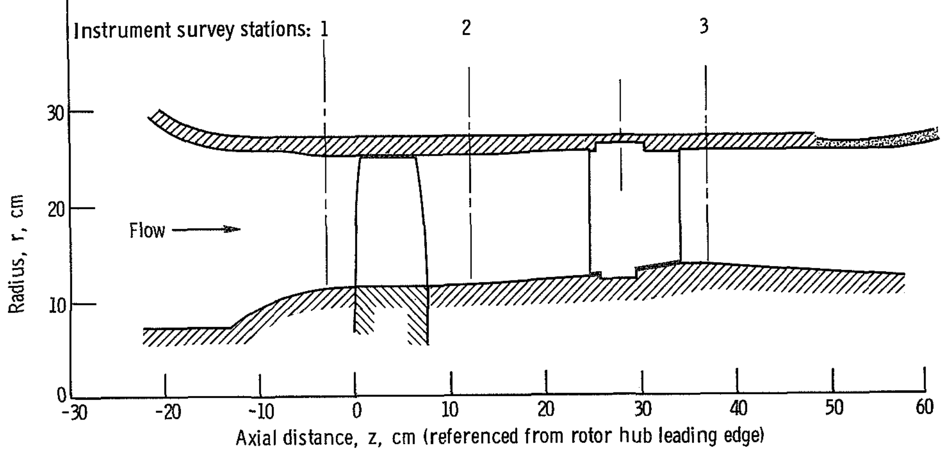

Figure 1. - STOL fan stage 55 flow path.

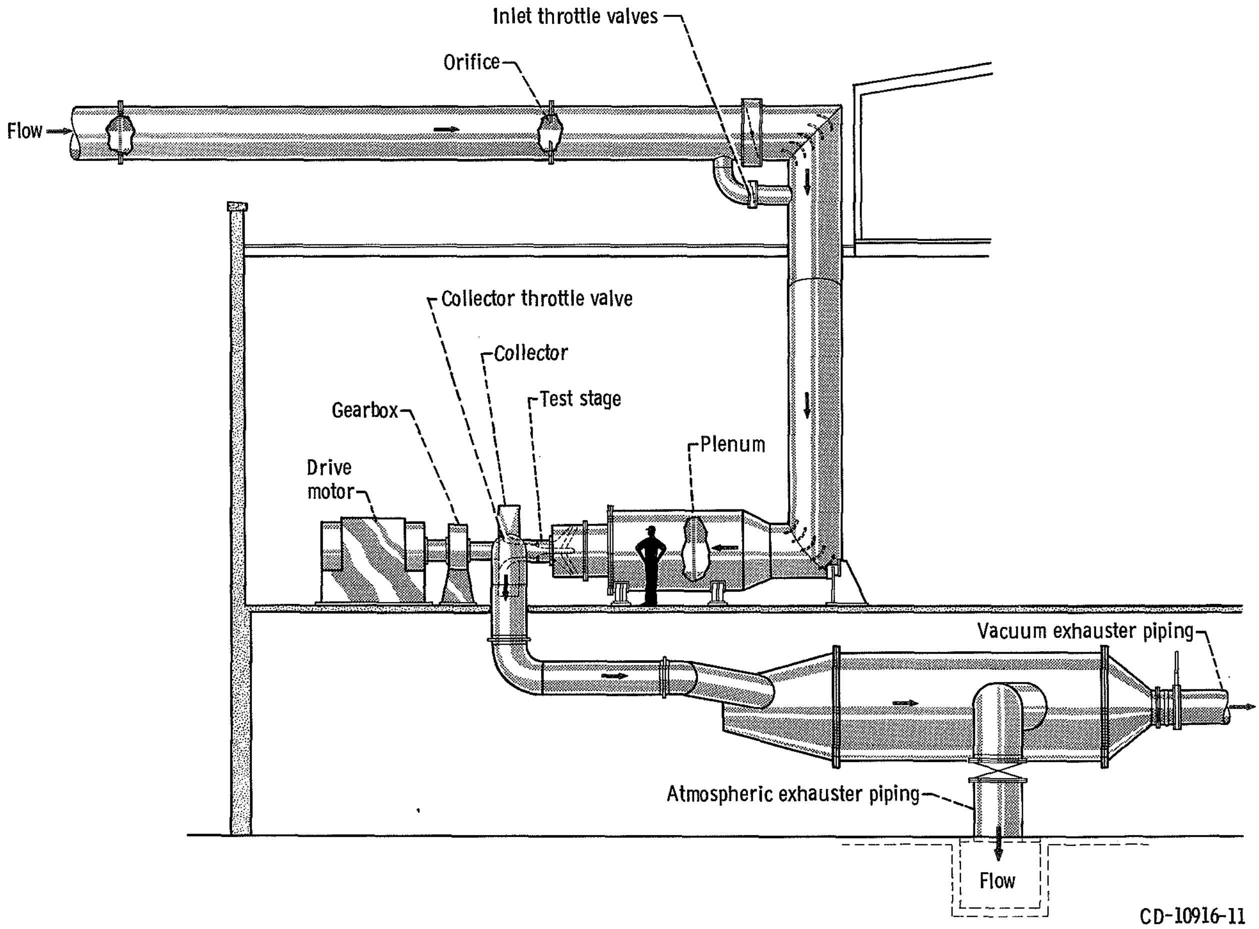

Figure 2. - Single-stage compressor facility.

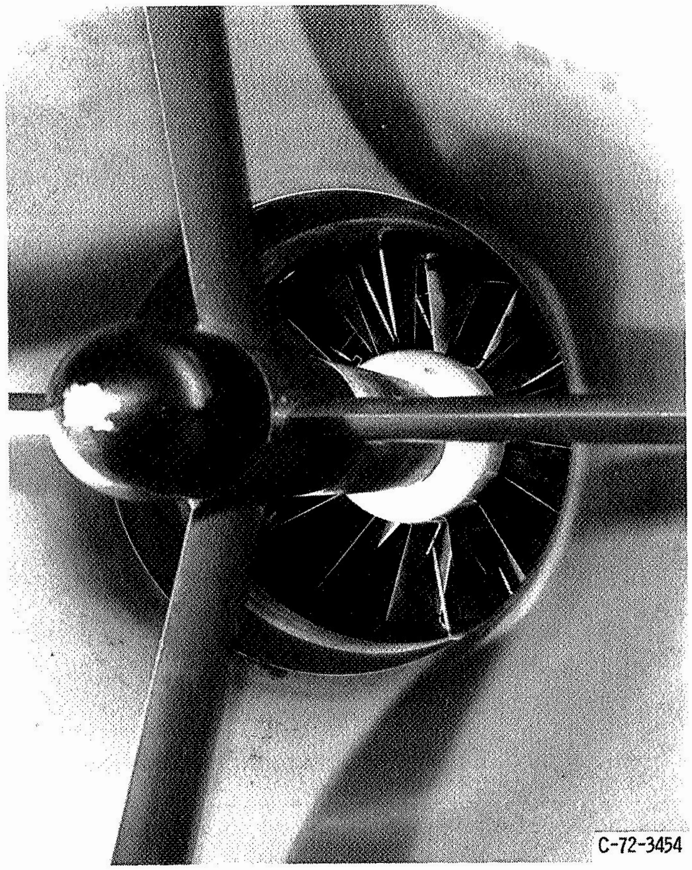

Figure 3. - STOL fan-stage 55 in compressor research facility.

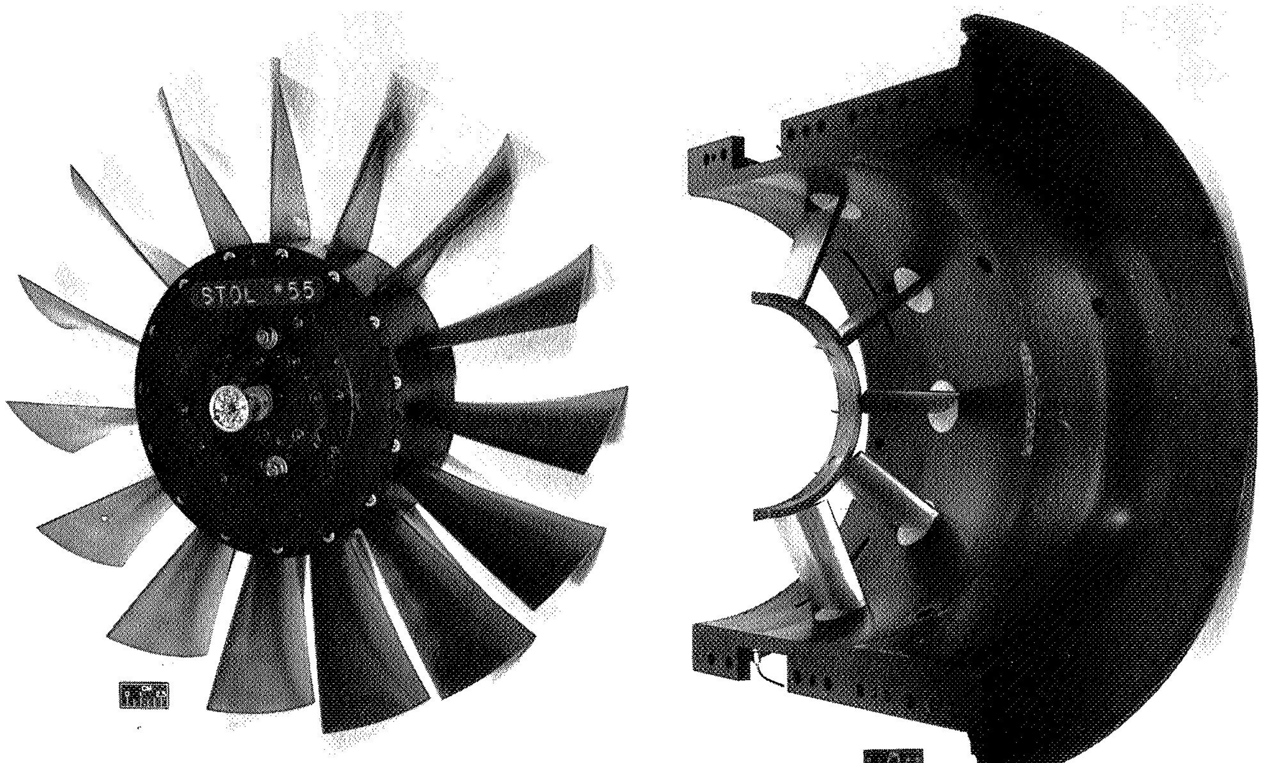

C-72-3909

C-72-3907

(a) STOL rotor 55.

(b) STOL stator 55.

Figure 4. - STOL fan-stage 55-55.

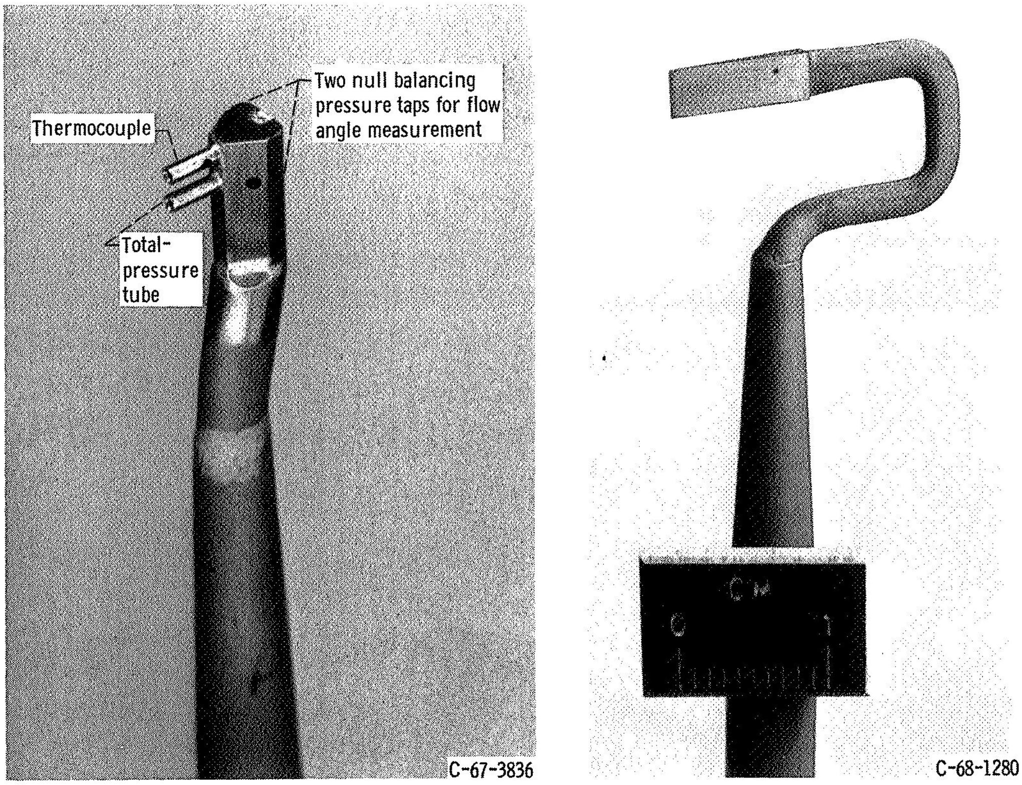

(a) Combination total pressure, total temperature, and flow angle probe.

(b) Static-pressure probe; 8° C-shaped wedge.

Figure 5. - Survey probes.

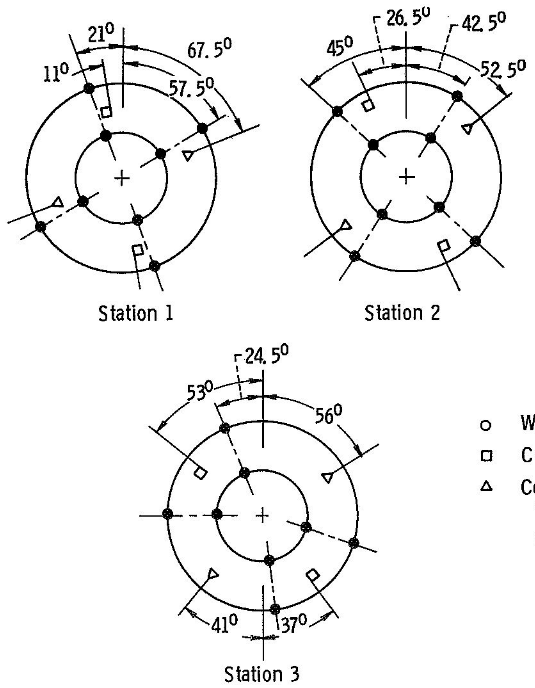

○ Wall static pressure
□ C-shaped static probe
△ Combination total pressure, total temperature, and angle probe

Figure 6. - Circumferential location of survey instrumentation at each station looking downstream.

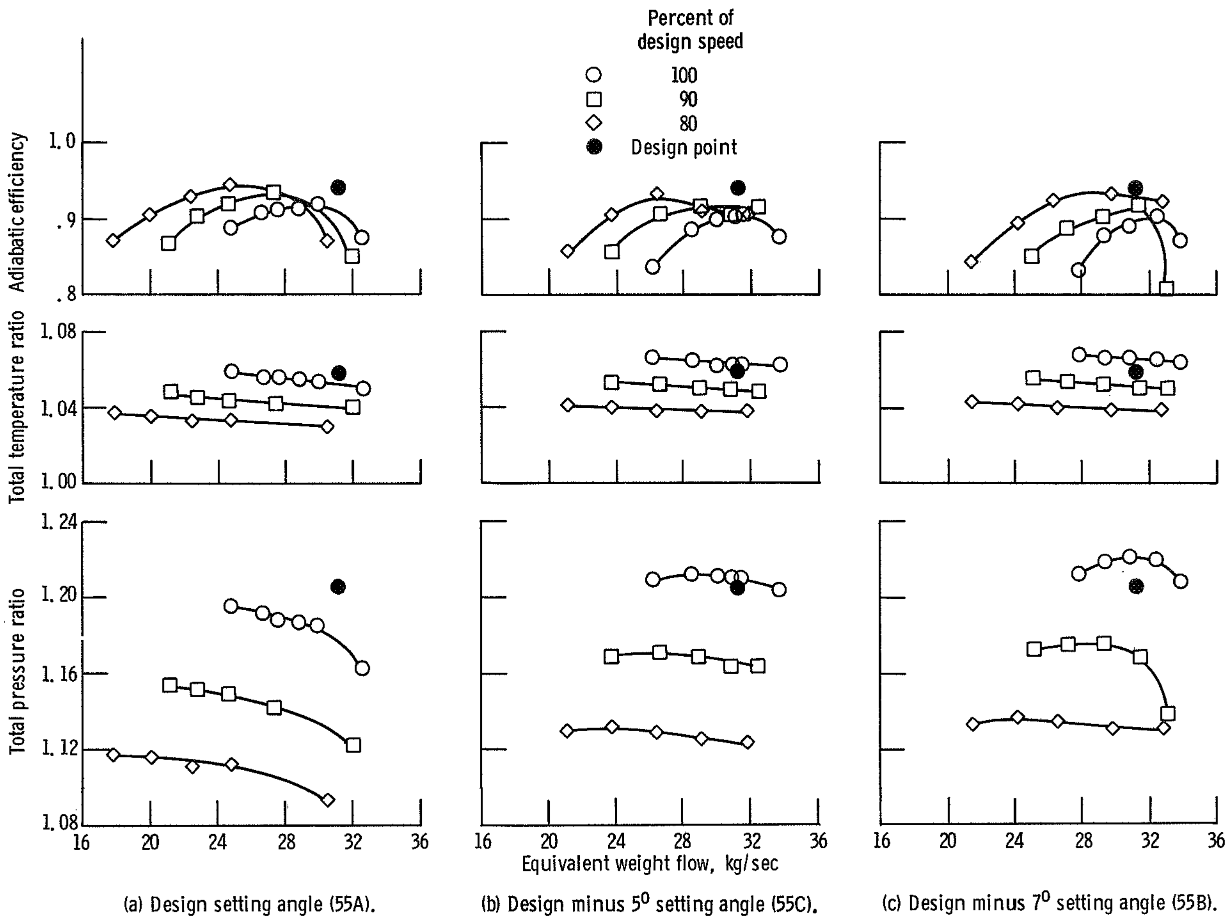

Figure 7. - Overall performance for rotor 55 at three different blade setting angles.

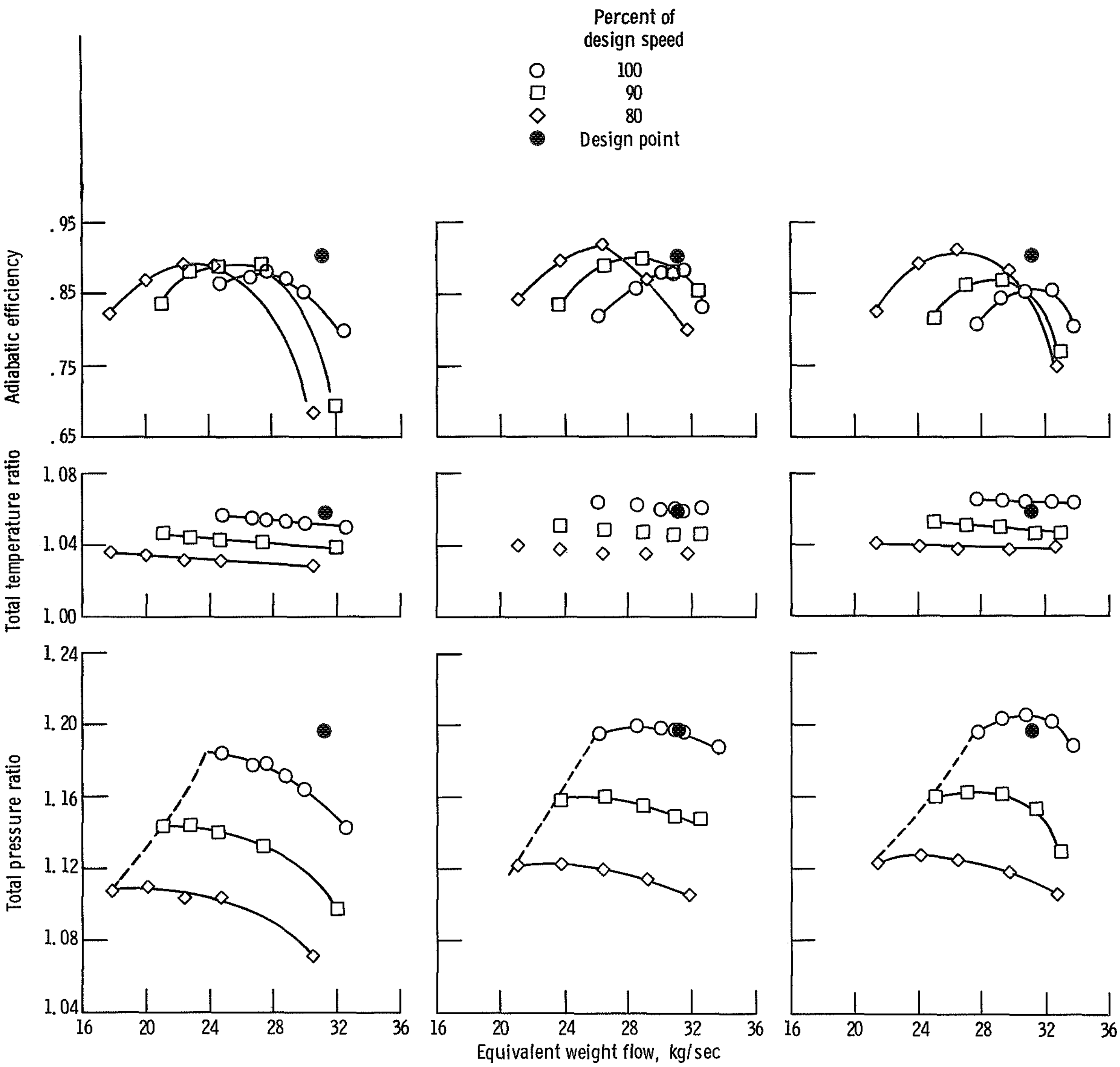

(a) Design setting angle (55A). (b) Design minus 5° setting angle (55C). (c) Design minus 7° setting angle (55B).

Figure 8. - Overall performance for STOL fan stage 55 at three different rotor blade setting angles.

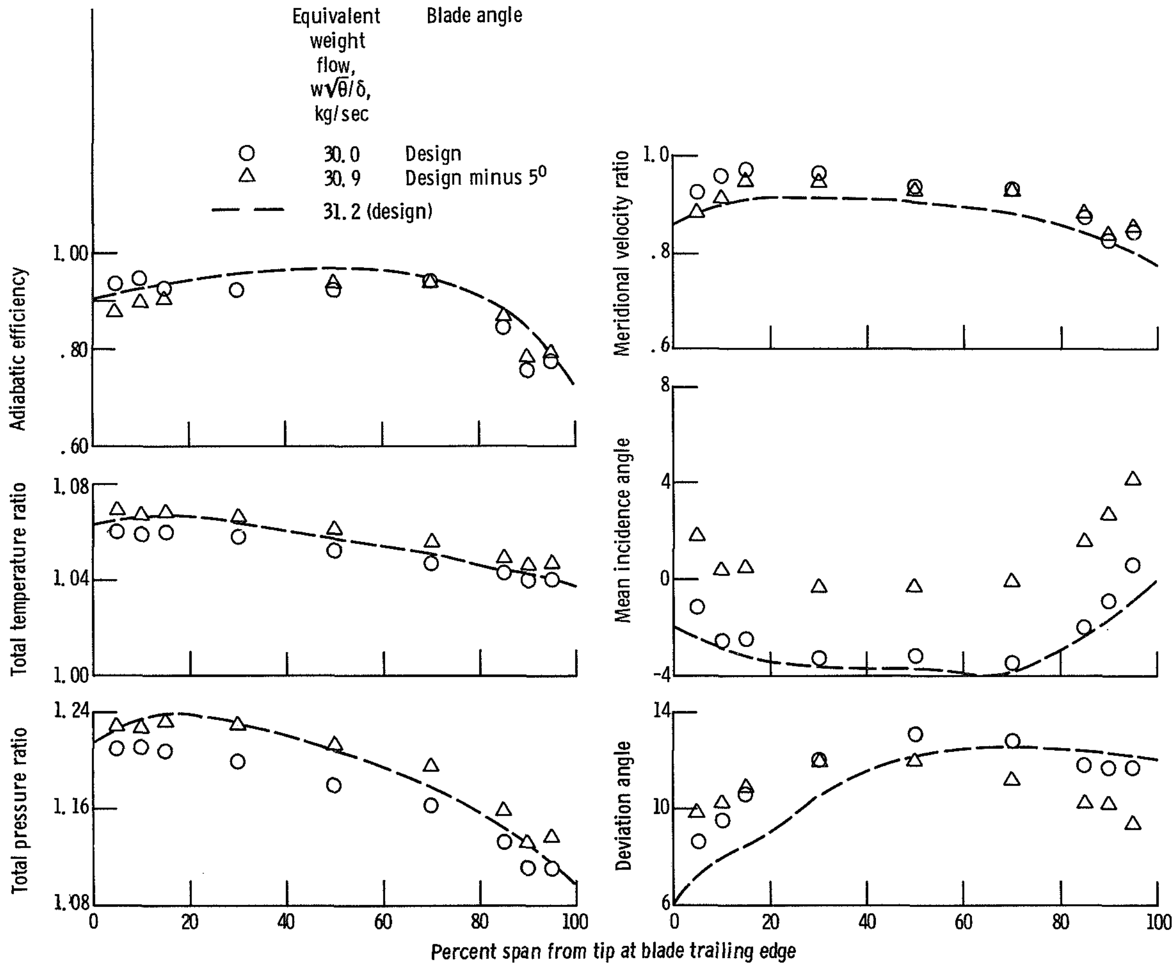

Figure 9. - Radial distribution of rotor performance at design speed and peak efficiency at two rotor blade setting angles.

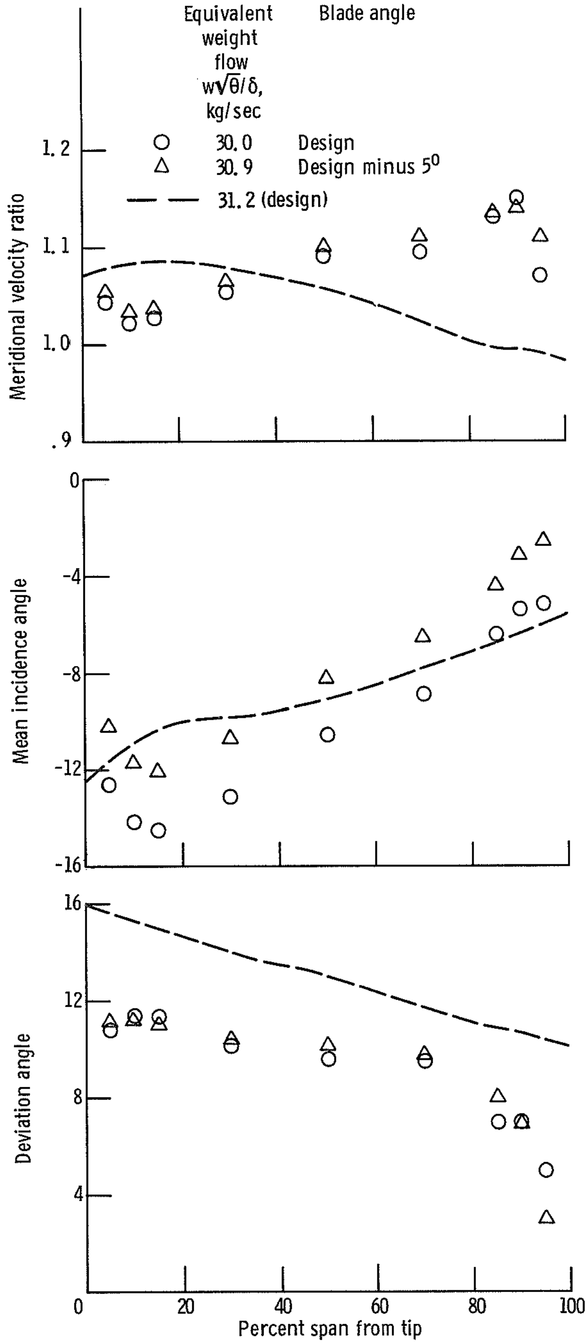

Figure 10. - Radial distribution of stator flow parameters at design speed and peak efficiency at two rotor blade setting angles.

NASA-Langley, 1973 —— 28 E-7434

NATIONAL AERONAUTICS AND SPACE ADMINISTRATION
WASHINGTON, D.C. 20546

OFFICIAL BUSINESS
PENALTY FOR PRIVATE USE $300

SPECIAL FOURTH-CLASS RATE
BOOK

POSTAGE AND FEES PAID
NATIONAL AERONAUTICS AND
SPACE ADMINISTRATION
451

U.S.MAIL

POSTMASTER: If Undeliverable (Section 158 Postal Manual) Do Not Return

"The aeronautical and space activities of the United States shall be conducted so as to contribute . . . to the expansion of human knowledge of phenomena in the atmosphere and space. The Administration shall provide for the widest practicable and appropriate dissemination of information concerning its activities and the results thereof."
—NATIONAL AERONAUTICS AND SPACE ACT OF 1958

NASA SCIENTIFIC AND TECHNICAL PUBLICATIONS

TECHNICAL REPORTS: Scientific and technical information considered important, complete, and a lasting contribution to existing knowledge.

TECHNICAL NOTES: Information less broad in scope but nevertheless of importance as a contribution to existing knowledge.

TECHNICAL MEMORANDUMS: Information receiving limited distribution because of preliminary data, security classification, or other reasons. Also includes conference proceedings with either limited or unlimited distribution.

CONTRACTOR REPORTS: Scientific and technical information generated under a NASA contract or grant and considered an important contribution to existing knowledge.

TECHNICAL TRANSLATIONS: Information published in a foreign language considered to merit NASA distribution in English.

SPECIAL PUBLICATIONS: Information derived from or of value to NASA activities. Publications include final reports of major projects, monographs, data compilations, handbooks, sourcebooks, and special bibliographies.

TECHNOLOGY UTILIZATION PUBLICATIONS: Information on technology used by NASA that may be of particular interest in commercial and other non-aerospace applications. Publications include Tech Briefs, Technology Utilization Reports and Technology Surveys.

Details on the availability of these publications may be obtained from:

SCIENTIFIC AND TECHNICAL INFORMATION OFFICE

NATIONAL AERONAUTICS AND SPACE ADMINISTRATION

Washington, D.C. 20546